Available online at www.sciencedirect.com
SCIENCE DIRECT®
Catalysis Today 86 (2003) 173–189
CATALYSIS TODAY
www.elsevier.com/locate/cattod

The effects of fluorine, phosphate and chelating agents on hydrotreating catalysts and catalysis

Mingyong Sun, Daniele Nicosia, Roel Prins*

Institute for Chemical and Bioengineering, Swiss Federal Institute of Technology (ETH), 8093 Zurich, Switzerland

Received 24 March 2003; received in revised form 16 May 2003; accepted 19 May 2003

Abstract

The effects of fluorine, phosphate and chelating agents on hydrodesulfurization (HDS) and hydrodenitrogenation (HDN) are reviewed. All three additives enhance the activity of $NiMo/Al_2O_3$ catalysts in HDN but have only a slightly positive or even a negative effect on the HDS activity of $CoMo/Al_2O_3$ and $NiMo/Al_2O_3$ catalysts. The positive effect on HDN is due to the enhancement of the hydrogenation of aromatic rings. On the other hand, these three additives diminish the rates of C–N bond breaking and alkene hydrogenation reactions.

All three additives are hard basic ligands that may interact strongly with hard acids such as coordinatively unsaturated Al^{3+} cations on the alumina surface. A strong interaction with the alumina support has several effects. First, molybdate and tungstate anions are no longer strongly bonded to the support and are predominantly present as polyanions, which can be easily sulfided to MoS_2 and WS_2 crystallites. The weaker interaction with the smaller support surface also leads to larger MoS_2 and WS_2 crystallites with a lower dispersion. Second, the Ni^{2+} and Co^{2+} cations will also interact more weakly with the alumina, and this makes the formation of Ni and Co promoter atoms in the catalytically active Ni–Mo–S and Co–Mo–S phases more efficient. Third, the weaker interaction of Mo and W with the support leads to a higher stacking of the MoS_2 and WS_2 crystallites and, thus, to the more active type II Ni–Mo–S and Co–Mo–S phases. The increased stacking is beneficial for geometrically demanding reactions such as the hydrogenation of aromatics. For less demanding reactions, such as alkene hydrogenation, aliphatic C–N bond breaking and thiophene HDS, the loss in dispersion is important.

Keywords: Hydrodesulfurization; Hydrodenitrogenation; Chelating agent

1. Introduction

In recent years, new legislation has led to a decrease in the amounts of sulfur and nitrogen in gasoline and diesel fuels and further decreases will be required in the coming years. As a consequence, research into the improvement of hydrotreating catalysts that remove sulfur and nitrogen atoms from oil fractions by hydrodesulfurization (HDS) and hydrodenitrogenation (HDN) has been intensified. Not only have the classic Co and Ni promoters of the supported MoS_2 and WS_2 catalysts attracted more attention, but also many types of additives. Three classes of additives, namely fluorine, phosphate and chelating agents, have been investigated extensively by industry and academia; fluorine and phosphate have been commercialized for many years. This chapter discusses these additives and how they improve the catalytic properties of hydrotreating catalysts. It took many years before the well-known promoting effects of these additives could

* Corresponding author. Tel.: +41-1-632-5490; fax: +41-1-632-1162.
E-mail address: prins@tech.chem.ethz.ch (R. Prins).

0920-5861/$ – see front matter © 2003 Elsevier B.V. All rights reserved.
doi:10.1016/S0920-5861(03)00410-3

be explained. As we will show, this was probably due to the fact that these additives do not interact with the catalytically active metal sulfides and that their effect is due to secondary effects, which make it difficult to elucidate their role. In the past decade opinions about the roles of these three additives have converged, and a valid overview of recent accomplishments is now possible.

2. The effect of fluorination of the alumina support

2.1. Effects on catalysis

Fluorine enhances the acidity of alumina and, therefore, improves its activity for acid-catalyzed reactions such as hydrocracking, which is used in removing sulfur, nitrogen and metal atoms from heavy feedstocks. Fluorine also has positive effects on HDS, which depend on the loading of fluorine and the composition of the catalysts. For instance, the thiophene HDS activity of $NiMo/Al_2O_3$ catalysts increased up to a fluorine loading of 3 wt.% [1,2], whereas the activity of $CoMo/Al_2O_3$ catalysts increased up to 0.8 wt.% F and decreased above 2 wt.% F [3–5]. The situation is also complex for tungsten-based catalysts. While Benitez et al. hardly observed an effect of fluorine on the thiophene HDS activity of NiW/Al_2O_3 catalysts [6], Song et al. found a maximum at 4 wt.% F [7]. This discrepancy may well be due not only to differences in Ni contents and calcination temperatures, but also to the different test conditions: Benitez et al. performed their HDS reaction at 2 MPa and Song et al. at 0.1 MPa. At low H_2 pressure, the rate-determining step may be the hydrogenation of the thiophene ring, while at high H_2 pressure hydrogenation is not rate-determining. As will be shown below, fluorine does indeed improve the hydrogenation properties of hydrotreating catalysts.

Fluorine also increased the HDS conversion of dibenzothiophene, 4-methyldibenzothiophene and 4,6-dimethyldibenzothiophene on $CoMo/Al_2O_3$ catalysts. It promoted the hydrogenation of the aromatic ring, the hydrogenolysis of the C–S bond and the migration of the methyl groups around the rings [8]. The increased migration of the methyl group was attributed to the increased acidity of the fluorinated catalysts. However, in an industrial hydrotreating process, HDS always occurs simultaneously with HDN. In that case, the acidic sites are occupied predominantly by nitrogen-containing compounds and are hardly available for the catalytic migration of the methyl groups. This is illustrated by the simultaneous reactions of cyclohexene and *o*-toluidine over an NiW/Al_2O_3 catalyst, in which methylcyclopentene and methylcyclopentane do not form [9]. Therefore, the use of more acidic catalysts to shift the methyl groups of 4,6-dimethyldibenzothiophene may not be the ideal solution in the deep HDS of oil fractions.

Fluorine also has a positive effect on HDN. In HDN, the hydrogenation of the nitrogen-containing heterocycle (as in pyridine) or of the aromatic ring, to which the nitrogen atom is attached (as in aniline), is essential if substantial removal of nitrogen is to occur. Only after this elimination of the aromaticity can the C–N bond be broken. Fluorine increased the HDN activity of W/Al_2O_3 and NiW/Al_2O_3 catalysts up to 1 wt.% F in the HDN of pyridine [6,10]. To understand how fluorine affects the HDN process, it is necessary to study its effect on the individual hydrogenation and C–N bond breaking reactions. For that reason, the effect of fluorine on the hydrogenation of the phenyl ring in *o*-toluidine and on the C–N bond breaking in 2-methylcyclohexylamine were investigated (Scheme 1) [9,11]. Fluorine affected the reactions of *o*-toluidine and 2-methylcyclohexylamine to different extents. While it significantly promoted the hydrogenation of *o*-toluidine to 2-methylcyclohexylamine, it had little effect on the HDN of 2-methylcyclohexylamine.

Not only is the removal of sulfur and nitrogen important in industrial hydrotreating, but also the hydrogenation of alkenes. Test reactions with cyclohexene showed that fluorine increases its conversion mainly by increasing the isomerization to methylcyclopentenes and methylcyclopentane on $NiMo/Al_2O_3$ [1], $CoMo/Al_2O_3$ [4] and W/Al_2O_3 [9] catalysts. The conversion to the hydrogenation product cyclohexane decreases, however. In the presence of *o*-toluidine, no isomerization products were detected due to the strong adsorption of the basic *o*-toluidine on the acid sites, and fluorine had little effect on the cyclohexene hydrogenation activities [9,11]. Similarly, the hydrogenation of the intermediate butenes in the HDS of thiophene decreased when fluorine was added to NiW/Al_2O_3 [6].

The influence of the time at which fluorine is added has been studied as well [11–13]. Matralis et al. found

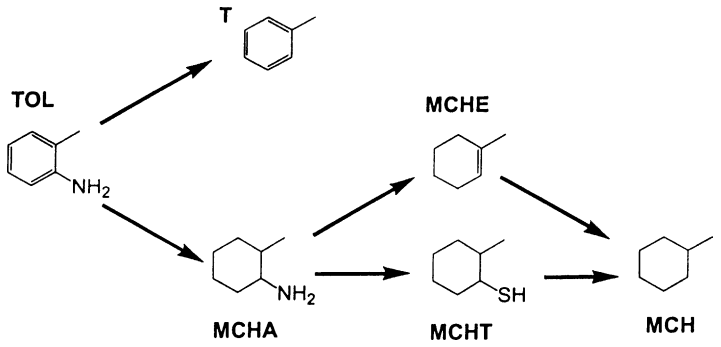

Scheme 1. HDN network of *o*-toluidine.

that, when fluoride was added after the impregnation of Co and Mo, the thiophene HDS activity was higher than when fluoride was added before Co and Mo [12]. Sarbak found the opposite result [13]. In the HDN of *o*-toluidine over Ni–Mo catalysts, the introduction of fluoride before Ni and Mo gave the more active catalyst [11]. In situ fluorination was also investigated by introducing fluorine as an organic fluorine-containing compound into the gas phase after preparing the catalyst in the sulfidic form. In situ fluorination increased both the elimination of nitrogen from 2-methylcyclohexylamine and the isomerization of cyclohexene but did not alter the hydrogenation of cyclohexene. Kinetic data indicate that the intrinsic properties of the active sites remain unchanged upon fluorination [14].

2.2. Explanations

Many explanations have been proposed for the effect of fluorine on hydrotreating reactions. For instance, the effect of fluorine has been attributed to an increase in acidity, to changes in the dispersion and distribution of the active MoS_2 or WS_2 phases, to their improved sulfidation and to a change in their morphology. As described above, the results obtained in different laboratories are not always consistent. Nevertheless, most investigations show that the promotional effect of fluorine on HDS and HDN increases with fluorine loading up to 1–3 wt.%, and that a further increase in fluorine loading results in lower activity.

The addition of fluorine to the alumina support increases its surface acidity and, thus, the activity for the acid-catalyzed reactions such as isomerization and cracking of hydrocarbons. This higher acidity, however, does not contribute directly to a higher HDN or HDS activity; in the presence of nitrogen compounds, the acidic sites are occupied by these basic compounds and are not available for the isomerization of cyclohexene [9]. While fluorination did not promote the C(sp^3)–N bond breaking, it improved the hydrogenation of the phenyl ring in *o*-toluidine. This indicates that the promotional effect of fluorine on the HDN activity is due to changes in the structure of metal sulfides rather than to a higher acidity.

The effects of fluorine on the reaction mechanism and the catalyst structure indicate that fluorine affects the catalytic performance by changing the metal sulfide phase rather than being directly involved in the hydrotreating reactions. To clarify the role of fluorine, it must be determined whether or not fluorine changes the intrinsic properties of the active sites or only their distribution. One way to answer this question would be to determine the number of active sites as well as their activity and to use the resulting turnover numbers to compare the catalyst activities. Unfortunately, there is no reliable method for determining the number of active sites of sulfide catalysts. On the other hand, one can determine the effects of fluorination on the rate and equilibrium adsorption constants as well as on the activation energy and heat of adsorption. Whereas rate constants include the number of sites, the other parameters depend only on the quality but not on the number of the sites. In this way, it was found that fluorine did not significantly change the activation energy and heat of adsorption of 2-methylcyclohexylamine and *o*-toluidine on the active sites [14,15]. These kinetic results indicate that fluorine does not change the

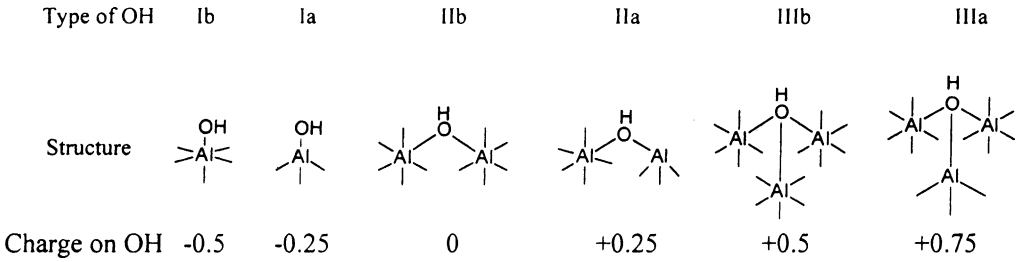

Scheme 2. Structure of hydroxyl groups on the surface of alumina.

nature of the active sites but changes the dispersion and distribution of the active phase.

How does fluoride change the morphology of the metal sulfide particles, when it does not have a direct interaction with them? Fluoride ions interact with the alumina support by replacing the hydroxyl groups on the support surface. Six types of hydroxyl groups, with slightly different net charges, exist on the surface of alumina (Scheme 2) [16,17]. Upon fluorination, fluoride ions preferentially displace the hydroxyl groups with the higher negative charge, often referred to as basic hydroxyl groups (Fig. 1). The total amount of hydroxyl groups on γ-alumina is around 1.4 mmol/g, and about 15% of the hydroxyl groups are basic. At low F loading, one fluoride ion replaces one hydroxyl group without destroying the bulk structure of the support. Above 3 wt.% F, which is equivalent to full substitution of the surface hydroxyl groups by fluoride ions, Al–O–Al linkages are broken to accommodate the extra fluoride ions. Finally, isolated $AlF_3{\cdot}xH_2O$ is formed at high fluorine loadings [18–20]. The dramatic decrease in surface area, caused by the destruction of the alumina bulk structure, is responsible for the decrease in catalytic activity at high fluorine loadings. ^{19}F magic-angle spinning NMR revealed three signals [18,20] of fluorine bonded to one, two and three octahedral aluminum atoms (Scheme 3) [18], corresponding to the displacement of types I, II and III hydroxyl groups, respectively (Scheme 2).

At low loading, the molybdate and tungstate anions also react preferentially with the basic hydroxyl groups on the alumina support [21–23]. The fluorination of the

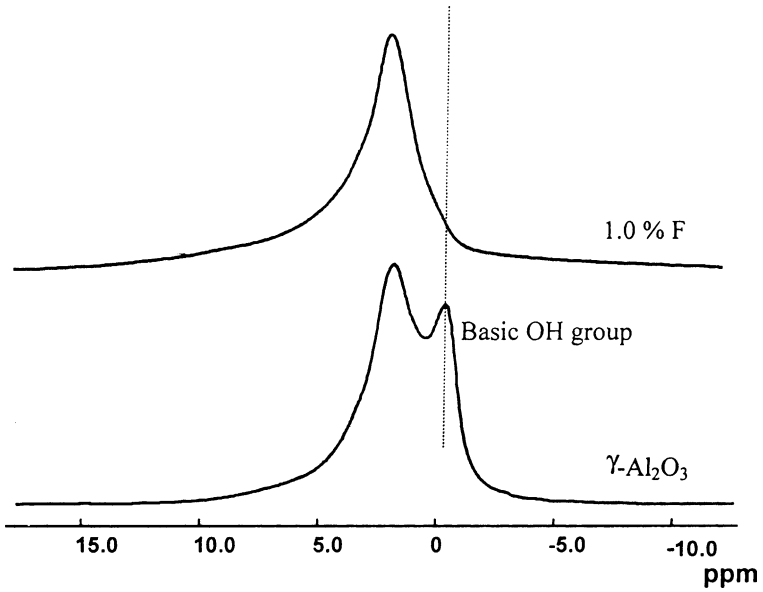

Fig. 1. Proton NMR of the OH groups of alumina.

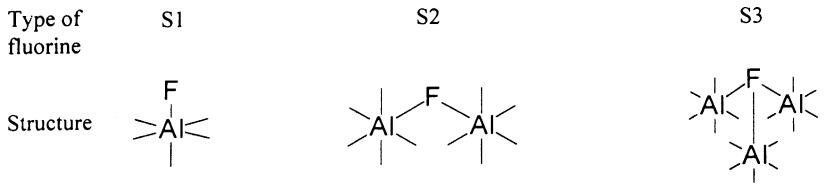

Scheme 3. Structure of fluoride groups on the surface of fluorinated alumina.

alumina support leaves very few basic hydroxyl groups and only a small number of non-basic hydroxyl groups for the metallate anions [18]. As a consequence, the metallate anions can only react with the small number of non-basic hydroxyl groups. In this way, fluorination of the alumina support weakens the metal–support interaction and leads to the formation of polymolybdate or polytungstate on the catalyst surface [7,24]. These polymetallates can be more easily sulfided and form stacked (multilayered) MoS_2 or WS_2. In agreement with these results, elemental analysis [6] and temperature-programmed sulfidation experiments [25] indicated a higher sulfur content in fluorinated samples, while transmission electron microscopy revealed that fluorine increased the number of WS_2 crystallites and their stacking [10,26,27]. In contrast to these observations, XPS measurements suggested that fluorination decreases the sulfidability of the active metals [2,5,6,25]. The incongruous XPS results must be due to the fact that XPS is a surface-sensitive technique, which mainly measures the metal atoms on the catalyst surface and is, thus, very sensitive to impurities and re-oxidation.

The more highly stacked WS_2 and MoS_2 particles are often assumed to be identical to the so-called type II phase of WS_2 and MoS_2, as defined by Candia et al. [28]. These authors observed that a classically prepared $CoMo/Al_2O_3$ catalyst has a lower intrinsic activity per surface Co atom than a catalyst, which was treated in H_2 and H_2S at higher temperature and referred to the first catalyst as structure type I and the second as type II Co–Mo–S [28,29]. Since then, many scientists consider the type I catalysts to consist of sulfidic M–MoS_2 particles (with M = Co or Ni promoter atoms located at the edges of the MoS_2 particles) with some Mo–O–Al linkages to the alumina. Type II M–MoS_2 particles are supposed to be fully sulfided, with only a weak van der Waals interaction with the support [30]. As a consequence, type II M–Mo–S particles have a higher degree of stacking than type I particles.

Daage and Chianelli proposed that the Mo atoms at the edges of the top layers of stacks of MoS_2 layers have a different activity than those of intermediate MoS_2 layers. From experiments with etched unsupported MoS_2, they deduced that only the top layers are active for the hydrogenation of dibenzothiophene, while the direct hydrogenolysis of the C–S bonds in dibenzothiophene to biphenyl occurs equally well on all MoS_2 layers [31]. Steric factors may explain the different reactivity. Adsorption in a σ mode ($\eta^1(S)$) should be possible at the edge Mo sites of all layers; this adsorption mode was assumed to be necessary for hydrogenolysis. On the other hand, π adsorption, with the aromatic ring parallel to the surface, results in hydrogenation; this geometry is unlikely on the Mo sites at the edges of the intermediate MoS_2 layers.

Quick EXAFS (QEXAFS) and quantitative EXAFS studies showed unequivocally that fluorine promotes the formation of WS_2 in the sulfidation of W/Al_2O_3 and NiW/Al_2O_3 catalysts (Fig. 2) [25,32]. Fluorine substantially decreased the W–O coordination number and increased the W–S and W–W coordination numbers corresponding to WS_2, demonstrating that fluorine facilitates the sulfidation of tungsten. The increase in the W–W coordination number upon fluorination indicates that fluorine induces the formation of larger WS_2 particles. Therefore, fluorine promotes the formation of well-developed MoS_2 and WS_2 with higher stacking and a larger particle size. These results are supported by studies of fully sulfided W/Al_2O_3 and NiW/Al_2O_3 catalysts prepared from $(NH_4)_2WS_4$ as the catalyst precursor. The addition of fluorine to such fully sulfided catalysts still increased the activity in the HDN of *o*-toluidine [9]. Thus, it is the change in the morphology and dispersion of MoS_2 or WS_2 on the support surface, rather than the extent of sul-

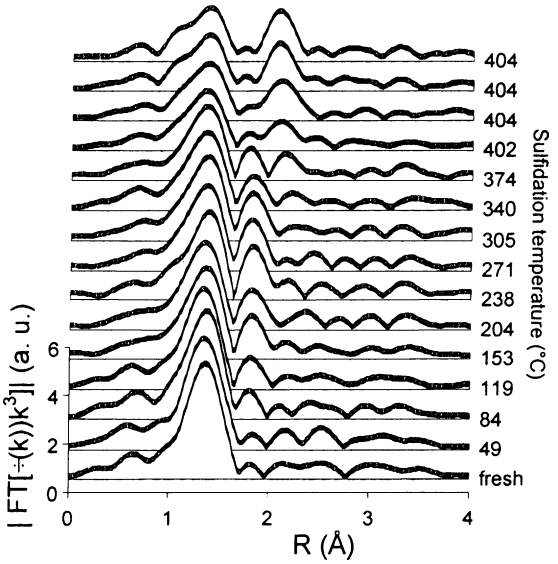

Fig. 2. Fourier transforms of the W L_{III} edge k^3-weighted QEXAFS of the sulfidation of NiW/Al_2O_3–F.

fidation, that affects the catalytic performance of the fluorinated catalysts.

The change in catalyst structure as a result of fluorination is reflected in a change in the catalytic performance. Although the hydrogenation of both alkenes and aromatics is believed to occur on sulfur vacancies, fluorine has different effects on these two hydrogenation reactions. While fluorination significantly promotes the hydrogenation of aromatic molecules, it has little effect on the hydrogenation of alkenes [1,4,6,9,11]. This indicates that the hydrogenation of the phenyl ring and the hydrogenation of alkenes occur on different catalytic sites. In agreement with this qualitative conclusion, the equilibrium adsorption constants of aromatic amines on the hydrogenation sites of alkenes are much smaller than those on the sites of the hydrogenation of the phenyl ring [33]. Aromatic molecules are supposed to be π bonded to a surface Mo or Ni atom and to take up a large amount of space, while one surface vacancy may be sufficient for the hydrogenation of alkenes [33,34]. The increase in the hydrogenation of aromatic rings due to fluorine addition is ascribed to the geometrically demanding aspect of this hydrogenation reaction. When single slabs of MoS_2 lie flat on the support, it is impossible for the aromatic ring to adsorb in a π mode on the Mo or Ni atoms at the MoS_2 edges. If, however, several MoS_2 slabs are stacked on top of each other, the aromatic ring is able to adsorb on edge sites of the upper MoS_2 slabs. Fluorination promotes the formation of larger and more highly stacked WS_2 and MoS_2 particles. This means that alkene hydrogenation and aliphatic C–N bond breaking, which are not very demanding reactions in terms of geometry, do not benefit from the fluorination. There may even be a negative influence through a loss of dispersion of the metal sulfide phase. The increased stacking at increasing fluorine loading has a positive influence on the highly demanding hydrogenation of aromatics, even though the dispersion decreases. Eventually, at high fluorine loading, the decrease in dispersion becomes so large that even the hydrogenation of aromatics becomes suppressed.

3. Effect of phosphate

An exhaustive review of the influence of phosphorus on the properties of alumina-based hydrotreating catalysts was published in 2000 [35]. Since then, few new insights have been reported; therefore, this section will be briefer than Sections 2 and 4. Only the most significant experimental results will be mentioned and their interpretation discussed. For further details we refer to [35] and references therein.

3.1. Effect of phosphate on the catalyst structure

Phosphorus is nearly always added as phosphoric acid to the support during wet catalyst preparation and in very few cases as ammonium phosphate. Phosphoric acid interacts strongly with the alumina support and forms an amorphous aluminum phosphate. Between 700 and 1000 °C this phosphate reacts with hydrogen to a Co, Ni or Mo phosphide [36]. This means that the aluminum phosphate is resistant to reduction during catalyst preparation and hydrotreating operation, during which the reduction temperature does not exceed 500 °C. Therefore, we will speak of the effect of phosphate rather than of phosphorus on hydrotreating reactions.

The interaction of phosphoric acid with the alumina is well documented. Scanning electron microscopy coupled with surface area and electrophoretic measurements demonstrated that the acid corrodes the alumina. It solubilizes some of the alumina, which,

after drying, leads to precipitation of $AlPO_4$ and loss of microporosity [37]. A non-homogeneous distribution of the $AlPO_4$ layer on the alumina surface is detected on the mm scale. ^{27}Al MAS NMR has confirmed the presence of amorphous aluminum phosphate [38]. IR [39] and NMR [23] investigations showed that the basic as well as the more abundant acid OH groups on the alumina surface (cf. Fig. 1) react with phosphoric acid. The acid OH groups, which are doubly or triply bonded to Al ions (type II or III in Scheme 2), react with phosphoric acid to a phosphate group bonded to one Al ion and to an OH group bonded to one or two of the other Al ions. This concurrent consumption of types II and III sites and generation of type I sites explains why the net consumption of the basic type I OH groups is much slower than expected because of their basicity [39]. The leveling off of the developing P–OH band indicates that, at higher concentrations of phosphoric acid, condensation to polyphosphate occurs, as confirmed by ^{31}P NMR measurements [38].

Upon adsorption of heptamolybdate on the γ-Al_2O_3 surface, at first only the basic OH groups react at a ratio of about one OH group per added Mo atom [21–23]. This indicates that molybdate is bonded by means of one oxygen atom to the support. At higher Mo loading, the acidic OH groups also disappear at a ratio of two OH groups to one Mo atom, suggesting that the Mo atoms are bonded to the support by two oxygen atoms. When a heptamolybdate solution is added to γ-Al_2O_3, previously impregnated with phosphoric acid and then calcined, both the basic and the acidic Al–OH groups and the P–OH groups react. At high Mo loading, the basic Al–OH and P–OH groups disappeared, but a substantial part of the acidic Al–OH groups remained. About two OH groups disappeared per added Mo atom, indicating that, with pre-impregnated phosphate too, the Mo atoms are bonded to the support through two oxygen atoms.

The addition of phosphate to the alumina surface not only decreases the surface area of the support and the number of basic sites, with which molybdate or tungstate can strongly react, but also decreases the point of zero charge of the surface [37]. As UV diffuse reflectance measurements demonstrated, this leads to a higher ratio of octahedrally to tetrahedrally coordinated Mo, i.e. more polymolybdate than molybdate is present on the phosphated support [40,41]. IR spectra indicate that isopolymolybdates (e.g. heptamolybdate) as well as heteropolymolybdates (e.g. phosphomolybdates and aluminomolybdate) form [42,43]. Temperature-programmed sulfidation indicated that the polymolybdates are easier to sulfide [41], and electron microscopy showed that the resulting MoS_2 particles are more highly stacked in the phosphate-containing $CoMoP/Al_2O_3$ and $NiMoP/Al_2O_3$ catalysts [44].

Diffuse reflectance spectra show that phosphate not only changes the structure of the molybdate anions, but also that of the Ni^{2+} or Co^{2+} cations. Phosphate decreases the number of tetrahedrally coordinated and increases the number of octahedrally coordinated Ni^{2+} cations in the oxidic $NiMo/Al_2O_3$ catalyst precursor phase [42]. These tetrahedrally coordinated Ni^{2+} cations are assumed to be located in a structure similar to the $NiAl_2O_4$ spinel structure on the alumina surface and are very difficult to retrieve and sulfide. When phosphate is present on the alumina surface, fewer Ni^{2+} ions are lost to the support and more are available for promoting the MoS_2 particles to form the highly active Ni–Mo–S phase.

Phosphate has the same effects on NiW/Al_2O_3 catalysts as on $NiMo/Al_2O_3$ catalysts. Thus, phosphate leads to fewer tetrahedrally coordinated Ni^{2+} ions [45], to polytungstate [45,46] and to higher stacking of WS_2 [46].

3.2. Effects on catalysis

Many groups have investigated the effect of phosphate on the HDS of thiophene. Some reported that the activity goes through a maximum with increasing phosphate loading [41,47,48], while others observed a continuous decrease only [49]. The decrease at high phosphate loading is due to the loss of surface area of the support and the concomitant loss of dispersion of the active sulfide phase. The diverging results at low phosphate loading may be due to the conditions under which the catalysts were prepared. Phosphoric acid interacts very strongly with the alumina support; unless special care is taken, the concentration of phosphate increases to a high level at the pore openings, where the impregnating phosphoric acid first comes into contact with the support. The phosphate on the alumina surface interacts with the molybdate during the subsequent impregnation with a molybdate solution, leading in turn to a non-homogeneous molybdate concentration [50]. Furthermore, the pH of the

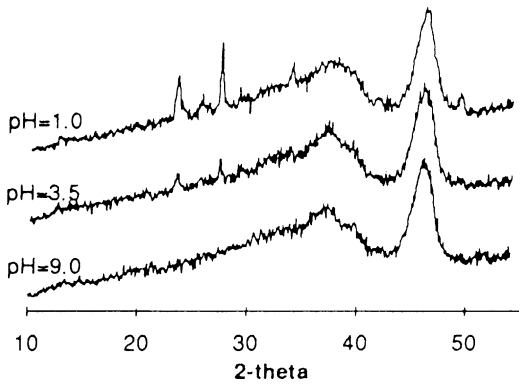

Fig. 3. Effect of the pH of the co-impregnation solution on the Mo dispersion in MoP/Al_2O_3 catalyst precursors. The sharp lines between 20 and 30° (2θ) are due to MoO_3.

impregnating solution is also important. If the pH is low, MoO_3 may precipitate, as demonstrated by XRD (Fig. 3) [51,52]. Finally, a high calcination temperature leads to a strong interaction between Ni and Co cations and molybdate anions with the support and to a decreased sulfidability and, thus, to a decrease in activity of the ultimate catalyst. When phosphate is used during catalyst preparation, it interacts strongly with alumina, leaving fewer surface sites to react with the metal ions. As a consequence, not as much Ni or Co and Mo is lost to the support. This explains why a catalyst procedure, in which phosphate is impregnated before Ni (Co) and Mo, results in more active catalysts.

Two studies addressed the effect of phosphate on the HDS of dibenzothiophene. One microflow study found that phosphate decreased the HDS activity of an $NiMo/Al_2O_3$ as well as $CoMo/Al_2O_3$ catalyst [30]. The other study, carried out in an autoclave with a $CoMo/Al_2O_3$ catalyst, showed that a phosphorus loading of 0.5% led to an activity increase of 35% in the HDS of dibenzothiophene as well as 4,6-dimethyldibenzothiophene [53].

While the effect of phosphate on the HDS of thiophene is, at best, only slightly positive and on the HDS of dibenzothiophene is, at best, positive for a Co–Mo catalyst in an autoclave, the effect on HDN is, without doubt, positive and strong. Studies with industrial feedstocks clearly demonstrated the positive effect [35] and studies with model compounds indicated that phosphate in particular promotes the hydrogenation of aromatic rings [47,49]. This hydrogenation of aromatic and hetero-aromatic rings is indeed the rate-determining step in most HDN networks. Other reactions that take place during HDN, such as the hydrogenation of alkenes and the breaking of C–N bonds in aliphatic molecules, are negatively influenced by phosphate [47].

3.3. Explanation

When oxidic samples, containing Co, Ni and Mo oxides and phosphate supported on Al_2O_3, are heated in hydrogen, Co, Ni and Mo phosphides are formed above 700 °C [36,54,55]. During the preparation and use of hydrotreating catalysts, the highest reduction temperature is only 500 °C; thus, it is unlikely that metal phosphides explain the effect of phosphate on hydrotreating catalysis. Furthermore, with the exception of nickel, all transition-metal sulfide catalysts supported on carbon are severely poisoned by phosphate [56]. Reduction to metal phosphide is probably much easier on carbon than on alumina, which interacts strongly with phosphate; it is, therefore, unlikely that metal phosphides are responsible for the promoting effect of phosphate, even though NiP [57] and MoP have a high activity in HDS and HDN [54,55].

The effect of phosphate is most probably due to a combination of factors. First, phosphate interacts strongly with the alumina support and not only reduces the surface area of the support, but also eliminates sites, with which the molybdate and tungstate ions may have interacted strongly. As a consequence, Mo and W will be present predominantly as polyanions, which can be sulfided more easily than the monoanions to the MoS_2 and WS_2 crystallites. The weaker interaction with the smaller support surface leads, on the other hand, to larger MoS_2 and WS_2 crystallites, as demonstrated by a decrease in oxygen chemisorption with increasing P content of a sulfided MoP/Al_2O_3 catalyst [41]. Second, since phosphate eliminated the stronger alumina surface sites, the Ni^{2+} and Co^{2+} cations also interact more weakly with the alumina. They can be more efficiently sulfided and form more Ni and Co atoms along the edges of the MoS_2 and WS_2 crystallites in the catalytically active Ni–Mo–S and Co–Mo–S phases. This may explain the maximum in NO adsorption and HDS activity of a Co–Mo catalyst at a loading of 0.5% P [53]. At a low P loading the efficiency of the catalytic use of Co increases with P loading, while above 0.5% P the dispersion

of MoS_2 and thus of Co at the edges decreases. A third factor, which explains the phosphate effect, is the higher stacking of the MoS_2 and WS_2 crystallites. The smaller surface area of the support and the weaker interaction of Mo and W with the support, due to the phosphate–support interaction, leads to a higher stacking of the MoS_2 and WS_2 crystallites and, thus, to the formation of the more active type II Ni–Mo–S and Co–Mo–S phases. Similar to the positive effect of fluorine addition on the hydrogenation of aromatic rings (Section 2.2), the positive effect of phosphate is ascribed to the demanding aspect of this hydrogenation reaction. The aromatic ring cannot adsorb in the π mode on the Mo or Ni atoms at the edges of single MoS_2 slabs. It can, however, adsorb on the edge sites of the upper MoS_2 slabs of stacked MoS_2 slabs. Thus, the increased stacking that occurs as a result of increasing phosphate loading positively influences the hydrogenation of aromatics. This explains why HDN was positively influenced by phosphate [35,47,49]. Dibenzothiophene undergoes HDS predominantly by direct C–S bond breaking, i.e. hydrogenolysis, and for less than 20% by hydrogenation of one of the aromatic rings, followed by C–S bond breaking. The (minor) hydrogenation path in the HDS of dibenzothiophene was promoted more than the hydrogenolysis path [53], as to be expected for enhanced stacking of the MoS_2 slabs. For 4,6-dimethyldibenzothiophene on the other hand, which reacts mainly by the hydrogenation path, phosphate promotes the hydrogenation path slightly less than the hydrogenolysis path. This needs further study. For reactions which are less demanding in the adsorption geometry, such as alkene hydrogenation, aliphatic C–N bond breaking and thiophene HDS, a loss of dispersion dominates.

4. Effect of chelating ligands

4.1. Introduction

Silica-supported catalysts tend to have a lower hydrotreating activity than alumina-based catalysts, which can be improved by using chelating ligands in their preparation. Chelating ligands are organic molecules that have two or more donor atoms, with which they can bind a metal cation and form a "chelate" (from the Greek *chelè*: claw). By adding chelating molecules to the impregnation solution, it is possible to prepare silica-supported catalysts, which have a similar or even higher activity than their commercial γ-Al_2O_3 counterparts in the hydrotreatment of gas oil. Chelating molecules, such as ethylenediaminetetraacetic acid (EDTA), nitrilotriacetic acid (NTA), 1,2-cyclohexanediamine-*N*,*N*,*N*′,*N*′-tetraacetic acid (CyDTA) and ethylenediamine (EN), were used. As early as 1986 a patent was issued for the use of such ligands [58]. It describes the pore-volume impregnation of a silica support with an ammonia solution of molybdate, an Ni or Co salt and the chelating ligand. After drying at 120 °C, the catalyst precursor is sulfided in flowing 5% H_2S/H_2 at about 350 °C. A calcination step is not performed so as to avoid destruction of the metal chelates. The resulting $NiMo/SiO_2$ catalyst, prepared with NTA as the chelating ligand, has an HDN activity that is nearly six times higher than that of conventionally prepared silica-based catalysts and even exceeds that of high quality commercial alumina-based hydrotreating catalysts. Since 1986, other patents have been published which report the use of chelating agents [59–61]. In 1998 the use of phosphate and glycol additives in the preparation of alumina-supported catalysts was patented as well [62]. In the latter case, the metal precursors, $CoCO_3$ and MoO_3, are dissolved in an acidic solution of H_3PO_4 at 80 °C and glycol is added. After pore-volume impregnation on γ-Al_2O_3, the oxidic catalyst precursor is dried at 120 °C and then sulfided.

Co^{2+}, Ni^{2+} ions and molybdate ions are usually added to porous supports, such as silica and γ-alumina, by pore-volume impregnation with an aqueous solution. After drying at 120–150 °C, the catalyst precursor is calcined at 400–500 °C to remove nitrate and ammonium counter ions in the form of NO_x and NH_3. This leads to Co, Ni and Mo ions in an oxidic state, and attached to the support. The interaction of the catalyst precursors with the support may be prevented by complexation of the metal ions. In this way, complete sulfidation and preparation of the most active type II Co–Mo–S phase are possible [63]. In the following sections, we will discuss the effects of chelating ligands on the impregnating solution, the oxidic catalyst precursor, the sulfided active catalyst and the catalytic activity, which are important in the preparation and testing of the catalyst.

4.2. The impregnating solution

The thermodynamic equilibria between molybdate and Ni^{2+} ions and chelating ligands, as a function of pH and the Ni:Mo molar ratio, predict that, in aqueous solution, NTA binds preferential with the Ni^{2+} or Co^{2+} ions. Thus, the $[Ni(NTA)(H_2O)_2]^{2-}$ complex is much more stable than $[MoO_3(NTA)]^{3-}$ (Fig. 4). UV-Vis and Raman measurements confirm these predictions [64]. Above a ratio NTA:Ni = 1 and in the pH range between 2 and 8, the NTA that is not bound to Ni^{2+} cations forms complexes with molybdate. For instance, in a solution containing Ni, Mo and NTA at a ratio of 1:2:2, all the Ni^{2+} ions and half the molybdate ions are complexed with NTA. The remaining Mo is present as heptamolybdate or molybdate anions. A bi-nuclear Co–Mo–NTA complex was not detected in the impregnating solution. Thus, the beneficial effect of NTA on the eventual catalyst is not due to the formation of such a bi-nuclear complex, as originally proposed by van Veen et al. [63]. When EDTA is used as a chelating ligand instead of NTA, the equilibrium composition changes only slightly. The main difference between NTA and EDTA is that Ni^{2+} or Co^{2+} cations can only bind one EDTA molecule. In addition to the amino acid chelates, several other complexing agents, such as ethylenediamine (EN) and other diamines, crown ether and organic acids were investigated [65]. All the agents improved the activity of an $NiMo/SiO_2$ catalyst in the HDS of thiophene.

Glycols behave differently than the other complexing agents because they are weakly chelating ligands. Thus, in a solution containing Co, Mo, triethylene glycol and phosphate, ^{13}C NMR and Raman showed that the triethylene glycol was not bonded to the Co^{2+} cations and that the Co^{2+} cations are present as free aquo complexes [66]. ^{31}P NMR and Raman demonstrated that Mo is present as the $P_2Mo_5O_{23}^{6-}$ phosphomolybdate anion.

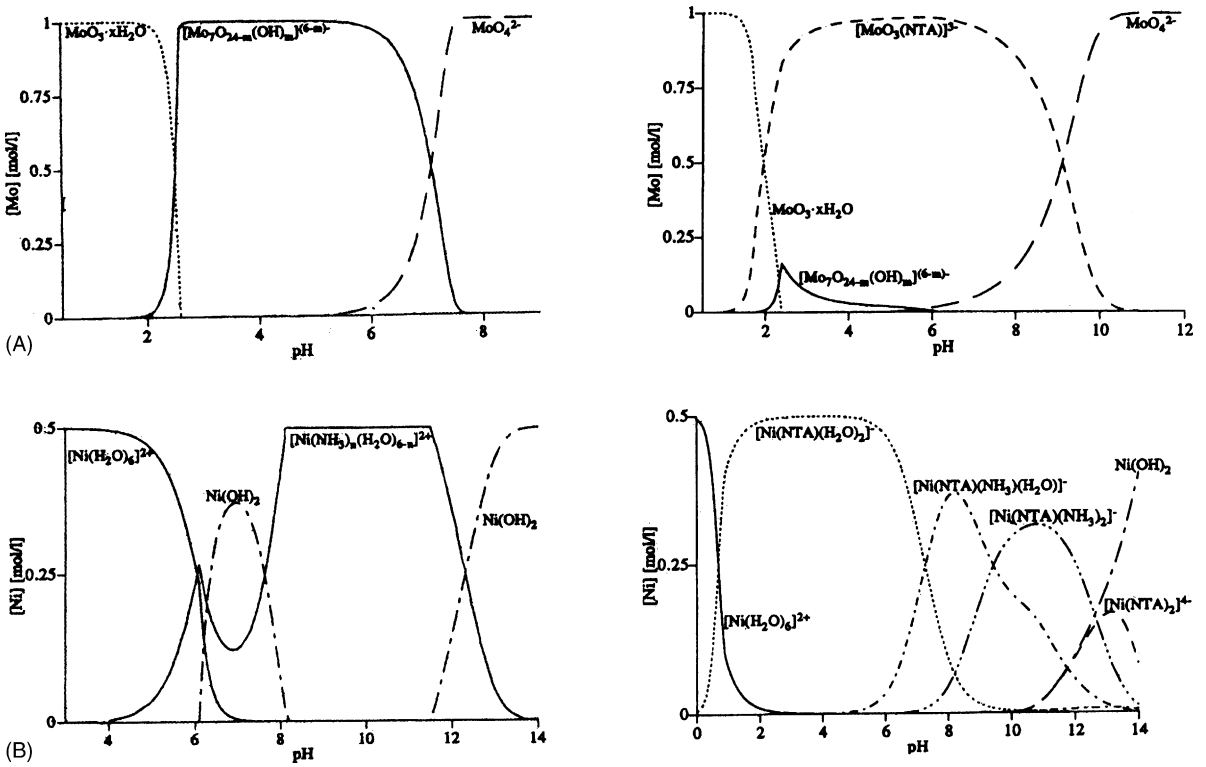

Fig. 4. Thermodynamic predictions of the Mo and Ni species in aqueous solution as a function of pH: (A) $[Mo]_{tot} = [NTA]_{tot} = 1$ mol/l; (B) $[Ni]_{tot} = [NTA]_{tot} = 0.5$ mol/l.

4.3. Impregnated support

In classic catalyst preparation, the support is impregnated with an aqueous solution of metal ions, and the resulting material is dried and calcined. When chelating ligands are used, the calcination step is omitted, because these organic compounds would otherwise be destroyed. In the absence of chelating ligands, the Ni^{2+} and Co^{2+} cations form aquo and amine complexes in the impregnating solution. During the drying of impregnated silica, the $Ni(NH_3)_x(H_2O)_{6-x}{}^{2+}$ complexes react with silanol groups, forming Ni phyllosilicate layers on the silica support [67]. Similar reactions occur during preparation of $NiMoEN/SiO_2$ catalyst precursors. Fig. 5 shows the Ni K-edge EXAFS of $NiMoEN/SiO_2$ catalyst precursors with different EN:Ni molar ratios [65]. The signal at 3 Å in the EN:Ni = 0 sample is due to a Si shell; it shows a strong Ni–support interaction. Larger amounts of EN cause a broadening of the Si shell in the Ni K-edge spectra. This means that the ligand led to a weaker interaction between the Ni^{2+} cations and the SiO_2 support. Nevertheless, an Ni–Si shell it still present at 3 Å, even at EN:Ni = 3.33, because oxygen atoms of the support replace only one or two coordinated EN molecules. When the EN/Ni molar ratio is substantially higher than six, however, Ni is fully coordinated by EN molecules and the EXAFS spectra no longer show a Si signal. In that case, EN inhibits the hydrolytic adsorption on the support and the formation of nickel silicate.

NTA behaves differently to EN. An Ni–Si interaction is observed only when there is insufficient NTA to complex all the Ni^{2+} cations. When there is enough NTA, the Co^{2+} and Ni^{2+} cations are present as isolated $[Co(NTA)(H_2O)_2]^-$ and $[Ni(NTA)(H_2O)_2]^-$ ions, respectively, on the support, as shown by Mössbauer experiments for a Co–Mo catalyst [63] and by reflectance UV-Vis, IR and EXAFS experiments for Ni-containing catalysts [64]. The difference between NTA and EN is due to the fact that NTA forms much more stable complexes than EN, protecting the Ni^{2+} and Co^{2+} cations better and hindering their interaction with the support.

As far as the Mo structure is concerned, the Raman spectra of a ligand-free sample indicate the presence of two Mo species, $Mo_7O_{24}{}^{6-}$ and $MoO_4{}^{2-}$ [64]. The

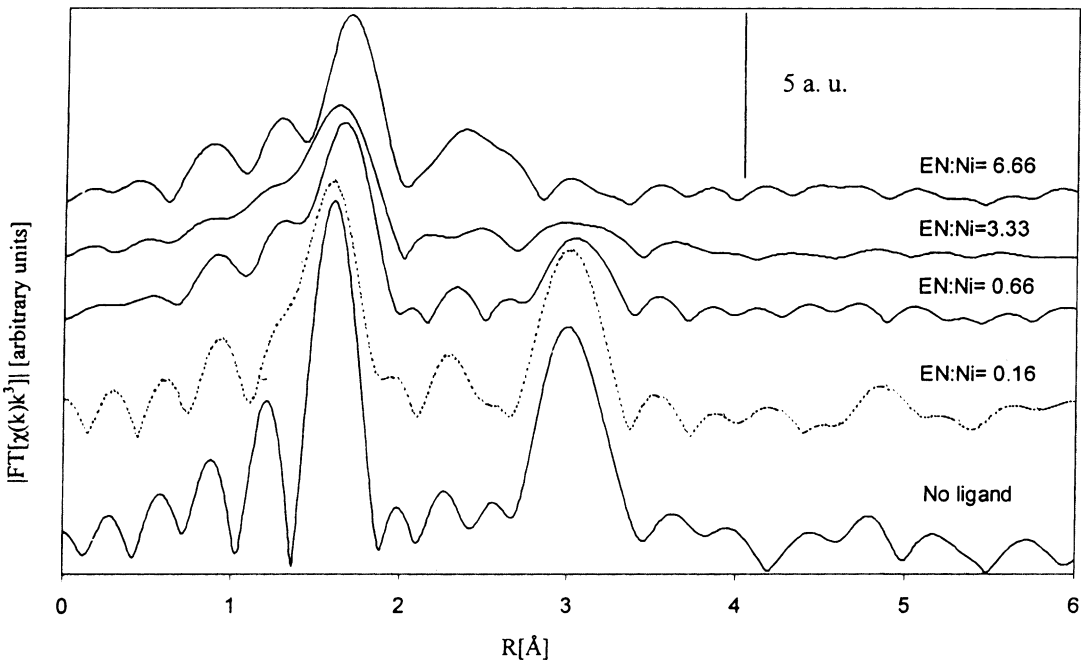

Fig. 5. Fourier transforms of the Ni K-edge k^3-weighted EXAFS of $NiMoEN/SiO_2$ catalyst precursors as a function of the ethylene diamine (EN) to Ni ratio.

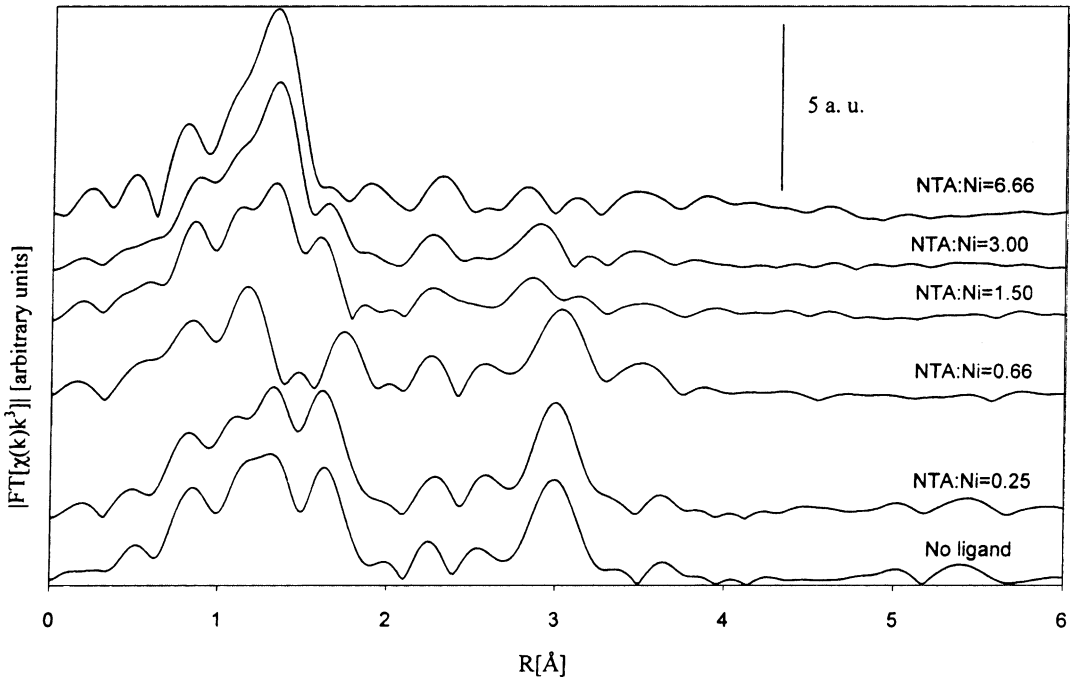

Fig. 6. Fourier transforms of the Mo K-edge k^3-weighted EXAFS of NiMoNTA/SiO_2 catalyst precursors as a function of the nitrilotriacetic acid (NTA) to Ni ratio.

Mo K-edge EXAFS spectra of NiMoEN/SiO_2 indicate that increasing amounts of EN do not have a strong effect on the Mo structure; in all cases a Mo–Mo shell at 3 Å is observed [65]. However, when NTA is used, the local Mo structure changes dramatically when the NTA:Ni ratio is increased from 0.66 to 1.5 (Fig. 6). At NTA:Ni $>$ 1 the Mo–Mo EXAFS contribution is no longer observed, because NTA is now available for complexing Mo to form $[MoO_3(NTA)]^{3-}$. As will be shown below, this decreases the HDS activity of the eventual catalyst.

While chelating ligands do not interact with silica, the situation is different with alumina. Glycol binds only weakly to Co^{2+} and Ni^{2+} cations, but may bind to the coordinatively unsaturated Al^{3+} sites on the γ-alumina surface, just as acetyl acetonate (acac) interacts strongly with such sites [68]. These acidic sites play a fundamental role in the anchoring of the metal precursors on the alumina surface. They interact very strongly with molybdate species, leading to the formation of the less active type I Co–Mo–S phase. The glycols probably prevent a strong metal–support interaction by blocking the coordinatively unsaturated alumina sites. In the presence of triethylene glycol, the Mo EXAFS spectrum of the oxidic CoMo/Al_2O_3 catalyst precursor showed a strong Mo–Mo peak at 3.7 Å, indicating that most of the Mo is present as polymolybdate [66]. In the absence of triethylene glycol this peak was considerably smaller, indicating that the polymolybdate partially decomposed to molybdate through interaction with the support. Since polymolybdate is known to give a better sulfidation, this would clarify the fact that glycols favor the formation of the more active Co–Mo–S II phase.

4.4. The sulfidation step and the sulfided catalyst

The sulfidation of the oxidic catalyst precursor is an essential step in the preparation of a hydrotreating catalyst, because the activity and structure of the working catalyst depend on the mode of sulfidation. In situ techniques, such as temperature-programmed sulfidation and QEXAFS, and ex situ techniques, such as Mössbauer emission spectroscopy and XPS, were used to investigate the sulfiding mechanism. The Mo XPS of a CoMo/SiO_2 sample showed that a contin-

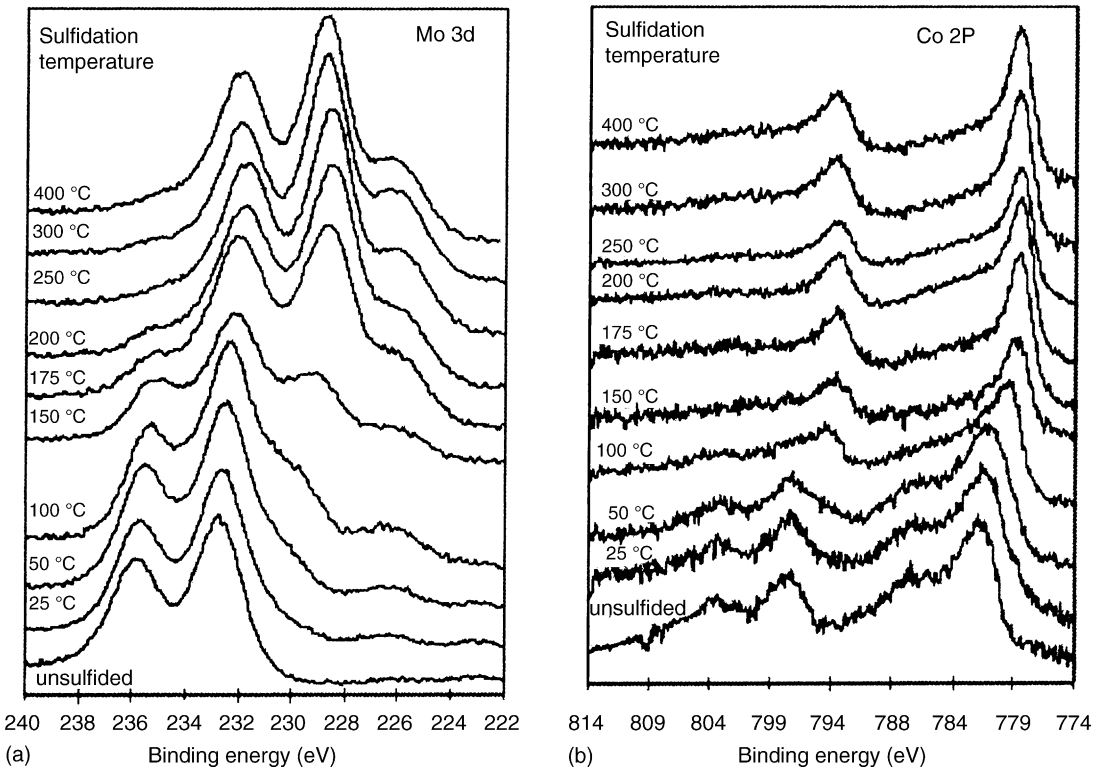

Fig. 7. Mo 3d (a) and Co 2p (b) XPS spectra of a calcined $CoMo/SiO_2/Si(1\,0\,0)$ model catalyst during sulfidation.

uum of Mo sulfidation states is obtained between 50 and 175 °C (Fig. 7a). In this temperature range, Mo is present in the oxidic VI, oxysulfidic V and fully sulfided IV states. Above 175 °C, Mo is fully sulfided [69]. The Co XPS of $CoMo/SiO_2$ (Fig. 7b) shows that the sulfidation of Co starts at 50 °C and is complete at 150 °C. Thus in a $CoMo/SiO_2$ catalyst, the sulfidation of Co is complete before that of Mo.

As discussed above, the chelating ligands interact strongly with Co or Ni ions, whereas Mo is unaffected. This leads to a retardation of the sulfidation of Co or Ni [69–71]. XPS spectra of Co/SiO_2 containing NTA proved that the sulfidation of cobalt starts at above 150 °C and is complete at 225 °C (Fig. 8a). NTA starts to decompose at the same temperature (Fig. 8b), enabling the sulfidation of Co. QEXAFS of the sulfidation of $NiMo/SiO_2$ catalyst precursors in the presence and absence of chelating ligands showed that the sulfidation can be divided into four temperature regions (Fig. 9) [71]. In the first region, Mo remained in the oxidic form. In the second region, Mo–O and Mo–S bonds co-existed up to 225 °C. The third region showed an intermediate phase, containing only Mo–S and Mo–Mo contributions, which might be similar to amorphous MoS_3. The fourth range, above 225 °C, represents fully sulfided MoS_2 [72]. The QEXAFS measurements showed that the temperature at which the Ni^{2+} cations are sulfided increases as the NTA:Ni ratio increases. Above NTA:Ni = 3, Ni is sulfided at about 270 °C. In EDTA-containing catalyst precursors, Ni is sulfided at about 350 °C; the same results were obtained for 1,2-cyclohexanediamine-*N*,*N*,*N*′,*N*′-tetraacetic acid (CyDTA) as the chelating ligand [73]. In catalyst precursors prepared in the presence of EN, Ni^{2+} cations are already sulfided at room temperature [71]. EN resembles glycol rather than NTA and EDTA.

4.5. Catalytic activity and explanations

All studies of the catalytic activity of silica-supported Co–Mo and Ni–Mo catalysts have shown that

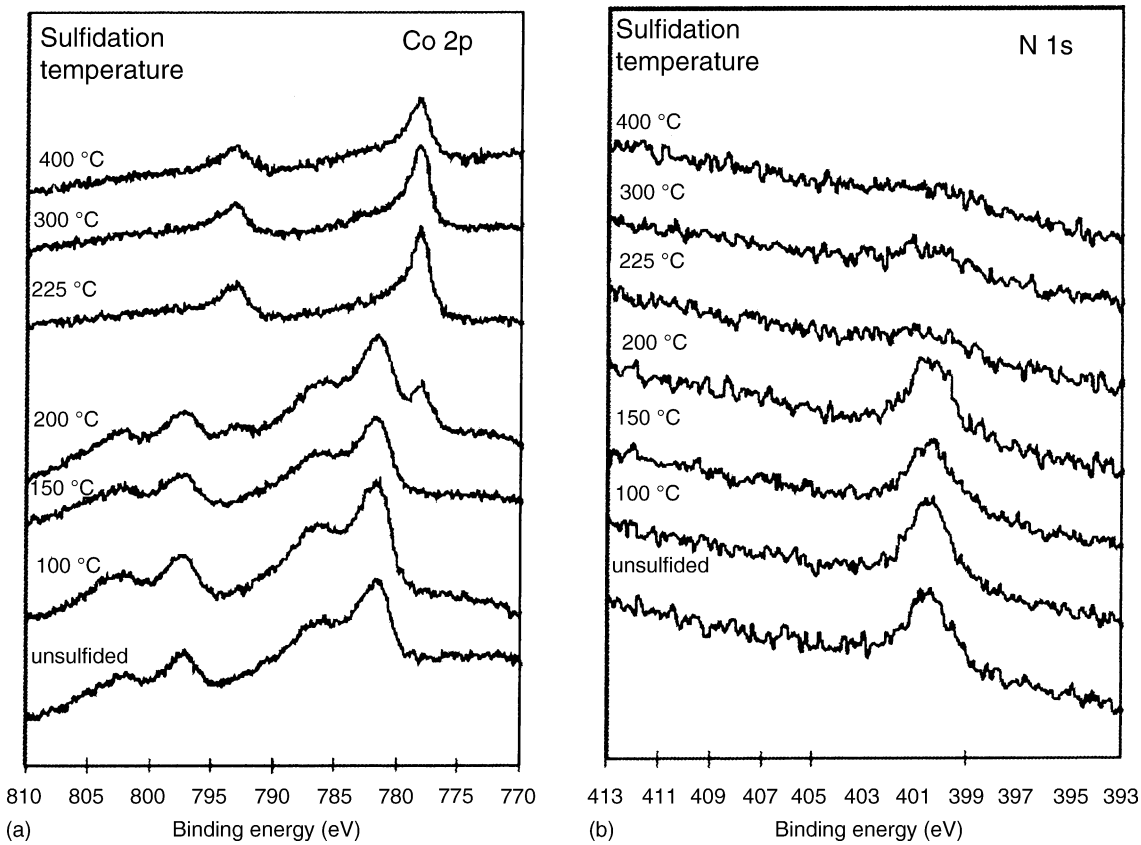

Fig. 8. Co 2p (a) and N 1s (b) XPS spectra of a calcined CoNTA/SiO_2/Si(1 0 0) model catalyst during sulfidation.

chelating ligands improve the hydrotreating activity. Section 4.4 showed that NTA and EDTA delay the sulfidation of Ni or Co, which occurs at a temperature at which all the Mo and W is fully sulfided to MoS_2 and WS_2 [64,69,71,73]. It was argued that, once the Ni and Co atoms are released by the chelating agent, they can move to the edges of the already formed MoS_2 and WS_2 and create the Co–Mo–S and Ni–Mo–S type II structures, which are the catalytically most active phases. Furthermore, NTA and EDTA prevent strong interactions between Ni^{2+} and Co^{2+} cations and SiO_2. The extent of the chelating effect and, therefore, the improvement of catalytic activity, depends strongly on the type and amount of the chelating ligand. If more NTA and EDTA is present than needed for the complexation of the Co^{2+} or Ni^{2+} cations, it starts to complex Mo; this leads to a decrease in the catalytic activity due to the poor sulfidation of Mo [65]. CyDTA has a higher complexing capability than NTA and EDTA and also leads to a higher thiophene HDS activity when used in the preparation of $CoMo/Al_2O_3$ catalysts [74]. While EDTA and NTA complex Co as well as Mo, CyDTA complexes only small cations such as Co^{2+}. Similar results were obtained in a study of the thiophene HDS activity of NiW/SiO_2 catalysts prepared in the presence of NTA, EDTA and CyDTA [73].

The effect of chelating ligands on the hydrotreating properties of alumina-supported catalysts has been studied in few cases only. van Veen et al. reported that $CoMo/Al_2O_3$ and $NiMo/Al_2O_3$ catalysts prepared in the presence of NTA are about 20% less active in the HDS of dibenzothiophene as the corresponding catalysts prepared without NTA. A positive result was obtained for the HDS of thiophene, while NTA hardly influenced the HDN of quinoline [30].

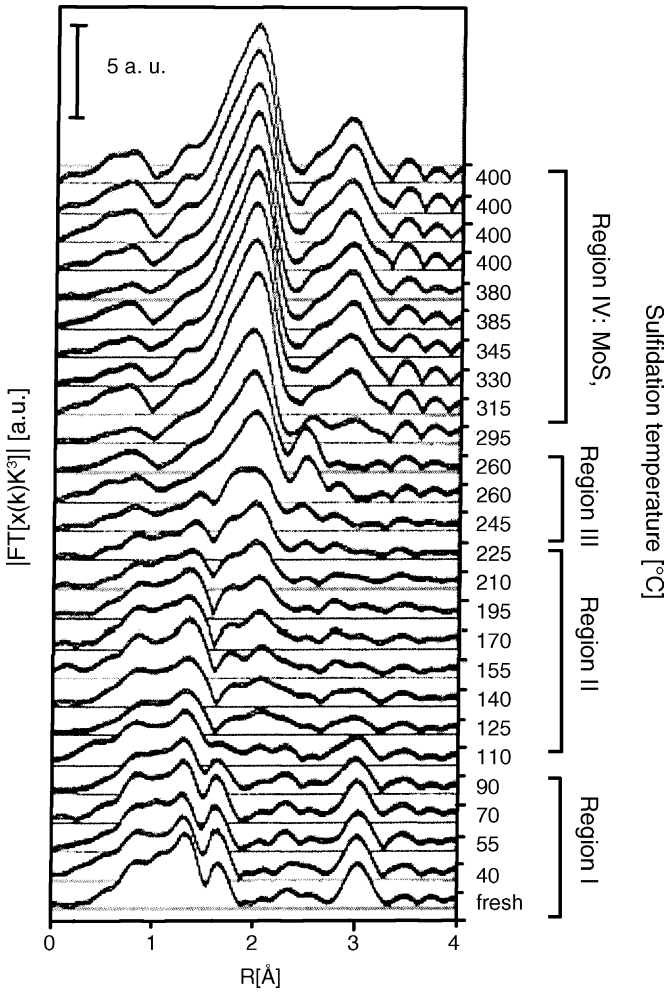

Fig. 9. Fourier transforms of the Mo K-edge k^3-weighted EXAFS of NiMo/SiO_2 catalyst precursors.

Cattaneo et al. reported that NTA strongly enhanced the activity of an NiMo/Al_2O_3 catalyst for the HDN of *o*-toluidine but hardly improved its activity in the HDS of thiophene [75]. NTA is believed to cause a decrease in the temperature of formation of the MoS_2 slabs, on which the hydrogenation of *o*-toluidine is enhanced. The ligands probably bring about a change in the sulfidation mechanism of Ni and a further high dispersion of the promoter. The different trends in the HDN and HDS reactions are explained by a difference in the rate-determining steps of these two reactions. In the HDN reaction, the hydrogenation of *o*-toluidine is the rate-determining step. This step is enhanced by the presence of more highly stacked MoS_2 crystallites, while for the HDS of thiophene the greater dispersion plays a more important role.

5. Conclusions

Fluorine, phosphate and chelating agents have very similar effects on hydrotreating catalysis. They all have a strong positive effect on HDN and a slightly positive or negative effect on HDS. In HDN, it is especially the hydrogenation of aromatic rings that is

promoted, while the hydrogenation of alkenes and the breaking of aliphatic C–N bonds is rather negatively influenced. Fluorine, phosphate and chelating agents have in common that they are hard basic ligands that interact strongly with hard acids such as coordinatively unsaturated Al^{3+} cations on the alumina surface and with the Ni^{2+} and Co^{2+} cations. The strong interaction with the alumina support leads to the following three effects. First, the additives reduce the surface area of the alumina and interact with sites, with which the molybdate and tungstate ions could have interacted strongly. As a consequence, Mo and W are predominantly present as polyanions, which can be more easily sulfided than the monoanions to the MoS_2 and WS_2 crystallites. At the same time, the weaker interaction with the smaller surface of the alumina leads to larger MoS_2 and WS_2 crystallites with a lower dispersion. Second, since the additives eliminated the stronger alumina surface sites, the Ni^{2+} and Co^{2+} cations also interact more weakly with the alumina. They can be more efficiently sulfided and form more Ni and Co atoms along the edges of the MoS_2 and WS_2 crystallites in the catalytically active Ni–Mo–S and Co–Mo–S phases. Third, the smaller surface area and the weaker interaction of Mo and W with the support leads to a higher stacking of the MoS_2 and WS_2 crystallites and, thus, to the formation of the more active type II Ni–Mo–S and Co–Mo–S phases. The increased stacking is beneficial for aromatics hydrogenation. For less demanding reactions, like alkene hydrogenation and aliphatic C–N bond breaking, the loss of dispersion dominates. The HDS of thiophene seems to occupy an intermediate position. At low fluoride or phosphate loading, the better sulfidability and incorporation of the Ni and Co promoter atoms into the MoS_2 edges enhance the HDS activity. At higher loading, the loss of dispersion decreases the activity.

The strong interaction between chelating ligands such as NTA and EDTA and Ni^{2+} and Co^{2+} cations is especially important for silica-supported catalysts. These interactions have two positive consequences. On the one hand, they prevent strong metal–support interactions that would make it difficult to sulfide the Ni and Co promoter ions. On the other hand, the strong interaction between chelate ligand and metal ion leads to a sulfidation of Ni and Co at higher temperature than that of Mo or W, so that the Ni–Mo–S and Co–Mo–S type II structures can be formed more easily.

Phosphate is in commercial use for many years, and fluorine is used for special hydrotreating processes. Apart from the combination phosphate-glycol, chelating agents do not seem to have been commercialized. The reason for this might be that phosphate has the advantage that it binds strongly to the alumina and is not stripped by traces of water, as is the case with fluorine. This may also explain why fluorine is added continuously during commercial operation. Chelating agents are more expensive than the other two additives and are lost during the sulfidation of the catalyst precursor. From the point of view of repeated use after regeneration, phosphate might also prove to be the additive of choice.

References

[1] K. Jiratova, M. Kraus, Appl. Catal. 27 (1986) 21.
[2] Ch. Papadopoulou, A. Lycourghiotis, P. Grange, B. Delmon, Appl. Catal. 38 (1988) 255.
[3] G. Muralidhar, F.E. Massoth, J. Shabtai, J. Catal. 85 (1984) 44.
[4] P.M. Boorman, R.A. Kydd, Z. Sarbak, A. Somogyvari, J. Catal. 106 (1987) 544.
[5] H.K. Matralis, A. Lycourghiotis, P. Grange, B. Delmon, Appl. Catal. 38 (1988) 273.
[6] A. Benitez, J. Ramirez, J.L.G. Fierro, A. López Agudo, Appl. Catal. 144 (1996) 343.
[7] C.J. Song, C. Kwak, S.H. Moon, Catal. Today 74 (2002) 193.
[8] C. Kwak, J.J. Lee, J.S. Bae, K. Choi, S.H. Moon, Appl. Catal. A 200 (2000) 233.
[9] M. Sun, M.E. Bussell, R. Prins, Appl. Catal. 216 (2001) 103.
[10] A. Benitez, J. Ramirez, A. Vazquez, D. Acosta, A. López Agudo, Appl. Catal. 133 (1995) 103.
[11] L. Qu, R. Prins, Appl. Catal., to be published in 249 (2003).
[12] H. Matralis, Ch. Papadopoulou, A. Lycourghiotis, Appl. Catal. A 116 (1994) 221.
[13] Z. Sarbak, Appl. Catal. A 164 (1997) 13.
[14] L. Qu, R. Prins, J. Catal. 207 (2002) 286;
L. Qu, R. Prins, J. Catal. 210 (2002) 183.
[15] M. Sun, R. Prins, J. Catal. 201 (2001) 138.
[16] H. Knözinger, P. Ratnasamy, Catal. Rev.-Sci. Eng. 17 (1978) 31.
[17] A.A. Tsyganenko, P.P. Mardilovich, J. Chem. Soc., Faraday Trans. 92 (1996) 4843.
[18] W. Zhang, M. Sun, R. Prins, J. Phys. Chem. B 106 (2002) 11805.
[19] S.M. Davis, G.D. Meitzner, D.A. Fischer, J. Gland, J. Catal. 142 (1993) 368.
[20] L. Fischer, V. Harlé, S. Kasztelan, J.B. d'Espinose de la Caillerie, Solid State Nucl. Magn. Res. 16 (2000) 85.
[21] O. Yasuaki, I. Toshinobu, J. Phys. Chem. 92 (1988) 7102.
[22] N.Y. Topsøe, H. Topsøe, J. Catal. 139 (1993) 631.

[23] H. Kraus, R. Prins, J. Catal. 164 (1996) 260.
[24] R.L. Cordero, J.R. Solis, J.V.G. Ramos, A.B. Patricio, A. López Agudo, Stud. Surf. Sci. Catal. 75 (1993) 1927.
[25] M. Sun, Th. Bürgi, R. Cattaneo, R. Prins, J. Catal. 197 (2001) 172;
M. Sun, Th. Bürgi, R. Cattaneo, D. van Langeveld, R. Prins, J. Catal. 201 (2001) 258.
[26] J. Ramirez, P. Castillo, A. Benitez, A. Vazquez, D. Acosta, A. López Agudo, J. Catal. 158 (1996) 181.
[27] M. Sun, P.J. Kooyman, R. Prins, J. Catal. 206 (2002) 368.
[28] R. Candia, O. Sørensen, J. Villadsen, N.Y. Topsøe, B.S. Clausen, H. Tøpsoe, Bull. Soc. Chim. Belg. 93 (1984) 763.
[29] H. Tøpsoe, B.S. Clausen, F.E. Massoth, Hydrotreating Catalysis, Springer, Berlin, 1996.
[30] J.A.R. van Veen, H.A. Colijn, P.A.J.M. Hendriks, A.J. van Welsenes, Fuel Proc. Technol. 35 (1993) 137.
[31] M. Daage, R.R. Chianelli, J. Catal. 149 (1994) 414.
[32] V. Schwartz, M. Sun, R. Prins, J. Phys. Chem. B 106 (2002) 2597.
[33] M. Sun, R. Prins, J. Catal. 203 (2001) 192.
[34] C. Moreau, C. Aubert, R. Durand, N. Zmimita, P. Geneste, Catal. Today 4 (1988) 117.
[35] R. Iwamoto, J. Grimblot, Adv. Catal. 44 (2000) 417.
[36] P.J. Mangnus, J.A.R. van Veen, S. Eijsbouts, V.H.J. de Beer, J.A. Moulijn, Appl. Catal. 61 (1990) 99.
[37] R. López Cordero, F.J. Gil Llambías, J.M. Palacios, J.L.G. Fierro, A. López Agudo, Appl. Catal. 56 (1989) 197.
[38] E.C. De Canio, J.C. Edwards, T.R. Scalzo, D.A. Storm, J.W. Bruno, J. Catal. 132 (1991) 498.
[39] J.M. Lewis, R.A. Kydd, J. Catal. 132 (1991) 465.
[40] R. López Cordero, N. Esquivel, J. Lázaro, J.L.G. Fierro, A. López Agudo, Appl. Catal. 48 (1989) 341.
[41] S.I. Kim, S.I. Woo, J. Catal. 133 (1992) 124.
[42] P. Atanasova, T. Halachev, Appl. Catal. 48 (1989) 295.
[43] A. Spojakina, S. Damyanova, L. Petrov, Z. Vit, Appl. Catal. 56 (1989) 163.
[44] R.C. Ryan, R.A. Kemp, J.A. Smegal, D.R. Denley, G.E. Spinnler, Stud. Surf. Sci. Catal. 50 (1989) 21.
[45] P. Atanasova, T. Tabakova, Ch. Vladov, T. Halachev, A. López Agudo, Appl. Catal. 161 (1997) 105.
[46] J. Cruz-Reyes, M. Avalos-Borja, R. López-Cordero, A. López Agudo, Appl. Catal. A 120 (1994) 147.
[47] M. Jian, R. Prins, Catal. Lett. 35 (1995) 193.
[48] J.M. Lewis, R.A. Kydd, P.M. Boorman, P.H. Van Rhyn, Appl. Catal. A 84 (1992) 103.
[49] S. Eijsbouts, J.N.M. van Gestel, J.A.R. van Veen, V.H.J. de Beer, R. Prins, J. Catal. 131 (1991) 412.
[50] J.L.G. Fierro, A. López Agudo, N. Esquivel, R. López Cordero, Appl. Catal. 48 (1989) 353.
[51] R. López Cordero, S. López Guérra, J.L.G. Fierro, A. López Agudo, J. Catal. 126 (1990) 8.
[52] M. Jian, R. Prins, Bull. Soc. Chim. Belg. 104 (1995) 231.
[53] C. Kwak, M.Y. Kim, K. Choi, S.H. Moon, Appl. Catal. A 185 (1999) 19.
[54] S.T. Oyama, X. Wang, Y.K. Lee, K. Bando, F. Requejo, J. Catal. 210 (2002) 207.
[55] C. Stinner, R. Prins, T. Weber, J. Catal. 202 (2002).
[56] S. Eijsbouts, J.N.M. van Gestel, E.M. van Oers, R. Prins, J.A.R. van Veen, V.H.J. de Beer, Appl. Catal. 119 (1994) 293.
[57] W.R.A.M. Robinson, J.N.M. van Gestel, T.I. Korányi, S. Eijsbouts, A.M. van der Kraan, J.A.R. van Veen, V.H.J. de Beer, J. Catal. 161 (1996) 539.
[58] M.S. Thompson, European Patent EP 0.181.035 A2 (1986).
[59] R.R. Chianelli, T.C. Ho, A.J. Jacobson, A.R. Young, European Patent EP 0.181.693 A1 (1986).
[60] T.C. Ho, L.E. McCandlish, A.R. Young, E.J. Osterhuber, US Patent 4,831,002 (1989).
[61] D.T. Eadie, M.A. Fefer, US Patent 5,122,258 A (1992).
[62] H. Yokozuka, S. Abe, T. Kamo, T. Suzuki, K. Uekusa, Y. Uragami, E. Yamaguchi, T. Yamaguhi, European Patent EP 0.601.772 B1 (1998).
[63] J.A.R. van Veen, E. Gerkema, A.M. van der Kraan, A. Knoester, J. Chem. Soc., Chem. Commun. (1987) 1684.
[64] L. Medici, R. Prins, J. Catal. 163 (1996) 28.
[65] R. Cattaneo, T. Shido, R. Prins, J. Catal. 185 (1999) 199.
[66] D. Nicosia, R. Prins, to be published.
[67] P. Burattin, M. Che, C. Luis, J. Phys. Chem. B 101 (1997) 7060;
P. Burattin, M. Che, C. Luis, J. Phys. Chem. B 102 (1998) 2722.
[68] J.A.R. van Veen, G. Jonkers, W.H. Hesselink, J. Chem. Soc., Faraday Trans. 85 (1989) 389.
[69] L. Coulier, V.H.J. de Beer, J.A.R. van Veen, J.W. Niemantsverdriet, Top. Catal. 13 (2000) 99.
[70] L. Coulier, V.H.J. de Beer, J.A.R. van Veen, J.W. Niemantsverdriet, J. Catal. 197 (2001) 26.
[71] R. Cattaneo, T. Weber, T. Shido, R. Prins, J. Catal. 191 (2000) 225.
[72] T. Weber, J.C. Muijsers, J.W. Niemantsverdriet, J. Phys. Chem. 99 (1995) 9144.
[73] G. Kishan, V.H.J. de Beer, J.A.R. van Veen, J.W. Niemantsverdriet, J. Catal. 196 (2000) 180.
[74] Y. Ohta, T. Shimizu, T. Honma, M. Yamada, Stud. Surf. Sci. Catal. 127 (1999) 161.
[75] R. Cattaneo, F. Rota, R. Prins, J. Catal. 199 (2001) 318.